Three-Dimensional Imaging of Cortical Structure, Function and Glioma for Tumor Resection

Tadashi Nariai, Michio Senda, Kenji Ishii, Taketoshi Maehara, Shinichi Wakabayashi, Hinako Toyama, Kiichi Ishiwata and Kimiyoshi Hirakawa

Department of Neurosurgery, Tokyo Medical and Dental University, School of Medicine and Positron Medical Center, Tokyo Metropolitan Institute of Gerontology, Tokyo, Japan

A three-dimensional brain imaging protocol with PET and MRI was used to visualize the cortical structure in relation to brain function and glioma infiltration to determine tumor resectability. **Methods:** Sixteen patients with glioma had a PET scan with ^{11}C-methionine to visualize tumor infiltration. The PET images were co-registered to the patients' own MRI reconstructed to the three-dimensional brain surface images to indicate the gyral structure and the extent of tumor infiltration. Thirteen patients, who bore tumors adjacent to the language or motor cortex, had $H_2{}^{15}O$ activation study to locate the eloquent cortex. The area of tumor infiltration was superimposed on the brain surface images together with the language and/or motor cortex. **Results:** When a tumor was located within a single gyrus without influencing surface cortical gyrus pattern, the motor and language areas were identified morphologically by three-dimensional surface image alone. However, when the tumor caused swelling and deformation of cortical structure, functional mapping with $H_2{}^{15}O$ activation technique was essential in locating them correctly. In such cases, the combined mapping of the facial motor area with oral movement and the language area with word repetition was the most useful method to identify the parasylvian structure in the dominant hemisphere. Total or near total resection of low-grade glioma in eight patients and the effective decompression of the active part of the malignant glioma in four patients was completed without causing functional neurological deterioration. **Conclusion:** The three-dimensional expression of cortical structure and function combined with PET glioma imaging with ^{11}C-methionine is useful for radical resection of cerebral glioma.

Key Words: glioma; activation study; three-dimensional image; PET carbon-11-methionine

J Nucl Med 1997; 38:1563–1568

Recent advances in computer image analysis have enabled the three-dimensional manipulation of tomographic images (*1*). Such techniques have been used to depict the brain structure three-dimensionally or to co-register images of different modalities such as PET and MRI (*2*). We have developed a three-dimensional brain imaging protocol that combines cortical surface imaging by MRI with functional brain map and tumor imaging by PET and applied it to the resection of glial tumors.

Although a number of clinical studies have indicated that the degree of initial resection of the glioma is one of the important prognostic indicators (*3–8*), it is often difficult to perform sufficient resection of gliomas. One of the difficulties is defining the area of glioma even during resection since tumor cells invariably infiltrate into apparently normal tissue (*9*). It is necessary to identify the area to be resected by preoperative imaging. For that purpose, we used PET ^{11}C-methionine imaging, which is superior to CT, MRI and SPECT in delineating gliomas (*10–12*).

Another factor that prevents maximal glioma resection is the need to protect cerebral functions. Although some functioning cortical areas can be defined by intraoperative electro-physiological technique (*13–16*), the characterization of its spatial relationship to the area of glioma, which infiltrates into apparently normal brain tissue, is difficult with an intraoperative survey alone. Accordingly, we evaluated a three-dimensional surface presentation of cortical structure in combination with mapping of cortical function using $H_2{}^{15}O$ activation technique to plan the extent of glioma resection.

METHODS

Sixteen patients with cerebral glioma were evaluated. Patient profiles are shown in Table 1. The patients had an MRI study on a 1.5 T super-conducting magnet system (Signa, General Electronics, Milwaukee, WI), and T1-weighted spin echo images were acquired in 3-mm thick contiguous axial sections without an interscan gap from the orbitomeatal line to the vertex.

The PET study was performed with a Headtome-IV scanner (Shimadzu Corp., Kyoto, Japan), providing 14 axial tomographic images with a center-to-center interval of 6.5 mm. The image spatial resolution was 7.0 mm FWHM. The patient's head was molded and fixed with a customized foam head holder (Smithers Medical Product Inc., Tullmadge, OH). The transmission data were acquired for attenuation correction with a rotating ^{68}Ge rod source. An arterial catheter was inserted into the radial artery for blood sampling. Cerebral blood flow (CBF) was measured under various conditions using the PET-autoradiographic method with an intravenous bolus injection of 1.0–1.5 GBq of ^{15}O-labeled water ($H_2{}^{15}O$) followed by a 2-min data acquisition (*17,18*). The arterial blood was sampled continuously to obtain the arterial time-activity curve.

During the CBF measurement, the patient gazed at a white dot projected on a monitor and either stayed at rest or performed one of the following tasks for functional mapping. In order to map the motor cortex in the hand area, a flexion-extension movement of fingers contralateral to the tumor was repeated (*19*). To map the motor cortex in the facial muscle and tongue area, a candy was put into the mouth and the patient was instructed to manipulate and taste it with the tongue and cheek. To map the language cortex, the patient was instructed to repeat words heard binaurally from a tape recorder (*20,21*). The CBF was measured under appropriate tasks determined for each patient as well as resting state, twice for each condition in a random order. The task started 30 sec before injection and continued to the end of data acquisition. A series of four to six scans was performed on each patient with a 10- to 15-min interscan interval. The global CBF was normalized to 50 ml/min/100 ml to remove fluctuation of global CBF (*22*). The average resting CBF image was subtracted from the average task

Received Jul. 12, 1996; accepted Nov. 27, 1996.

For correspondence or reprints contact: Tadashi Nariai, MD, Department of Neurosurgery, Tokyo Medical and Dental University, 1-5-45 Yushima, Bunkyo-ku, Tokyo 113, Japan.

TABLE 1
Patient Data

Patient no.	Age (yr)	Sex	Pathology of glioma	Location of glioma	PET activation	Resection	Postoperative result
1	17	M	G	Lt Tm	L & M (oral)	Total	No symptom
2	28	F	G	Lt Tm	NP	Total	No symptom
3	30	F	A	Rt Fr	M (finger & oral)	Total	Weakness of face and hand for 1 wk (fully recovered)
4	33	F	A	Lt Tm	L & M (oral)	Total	No symptom
5	37	M	A	Rt Par	M (finger)	Biopsy	Unchanged motor symptom
6	39	M	AA	Lt Tm	L	Near total	No symptom
7	39	M	A	Lt Fr	L & M (finger)	Biopsy	No symptom
8	40	M	A	Rt Tm	NP	Total	No symptom
9	45	M	O	Rt Tm	L	Near total	Dysphasia for 2 wk and fully recovered
10	46	F	GBM	Lt Tm-Par	L & M (oral & finger)	Subtotal	Amelioration of preoperative dysphasia and hand weakness
11	50	M	A	Rt Tm	NP	Total	
12	52	M	A	Rt Fr	M (finger & oral)	Biopsy	No motor deterioration
13	54	F	GBM	Lt Tm-Par-Occ	L & M (oral)	Partial	No deterioration of sensory dysphasia
14	56	F	AA	Rt Tm	L	np	(Language symptom +)
15	56	M	GBM	Lt Tm	L	Partial	No deterioration in alexia and agraphia
16	60	M	A	Lt Fr	M (finger)	Total	Weakness of foot and hand for 5 days (fully recovered)

G = ganglioglioma; A = astrocytoma (Grade 2); AA = anaplastic astrocytoma; O = oligodendroglioma; GBM = glioblastoma multiform; ICH = intracerebral hemorrhage; Fr = frontal; Tm = temporal; Par = parietal; Occ = occipital; L = language; M = motor; np = not performed.

image to obtain the CBF increase images for each task and for each patient.

After the completion of the activation study, ^{11}C-labeled L-methionine (450–550 MBq) was intravenously injected. Twenty minutes after the injection, the brain radioactivity distribution was measured for 10 min. The regional uptake of ^{11}C-methionine was expressed as the standardized uptake value (SUV) [or the differential absorption ratio (DAR)]. SUV = (tissue activity/ml)/(injected radioactivity/body weight (g)) (*10*). All the PET data were registered to the patient's MRI using a program developed in our institute (*23,24*) using the image analysis software system "Dr. View v 4.0" (Asahi Kasei Co. Ltd., Tokyo, Japan) and "AVS" (Advanced Visual System Inc., Waltham, MA) running on a workstation (Indigo2, Silicon Graphics Inc., Mountain View, CA). The three-dimensional brain surface images were reconstructed from axial MRI using a program developed in our institute (*25*). The area of tumor infiltration was defined as pixels that have elevated uptake of ^{11}C methionine in comparison to the surrounding cortex (threshold: SUV > 1.8–2.2 or tumor/cortex > 1.40–1.50, as determined by neurosurgeons). The eloquent cerebral cortex was defined as the area that exceeded a 10% or 15% (% global CBF) increase of CBF by the language or the motor task, respectively, on the subtracted CBF images. After the background noise was masked out, the tumor area and the eloquent cortical area were volume-rendered and superimposed on the brain-surface MR images.

RESULTS

Tumor Localization with Three-Dimensional Carbon-11-Methionine Images

MRI with Gd-DTPA indicated that the blood-brain barrier was not disrupted in the low-grade tumor of eight patients (Patients 2, 3, 4, 5, 7, 8, 9, 11) and in the anaplastic astrocytoma of one patient (Patient 14). In those cases, the ^{11}C-methionine PET image provided more convincing information than MRI in diagnosing and delineating the tumor. In two patients with localized glioma in a single gyrus (Patients 2 and 11), only the ^{11}C-methionine PET image could reveal the neoplastic nature of the lesion, and total removal was performed (Fig. 1). Two patients (Patients 1 and 6) had histories of intracerebral bleeding, and MRI could not distinguish the changes caused by tumor infiltration from those caused by bleeding. In these two patients, the tumor could be localized only by methionine-uptake PET images. In a recurrent case (Patient 13), ^{11}C-methionine was useful in distinguishing the area of recurrent tumor and that of radiation injury or tissue damage caused by the initial operation. In four other patients (Patients 10, 12, 15, 16), high methionine uptake extended beyond the area of the disrupted blood-brain barrier, as indicated by Gd-DTPA enhancement. The delineation of tumor with the ^{11}C-methionine PET image was more specific than T2-weighted MRI, distinguishing the active tumor invasion from secondary changes caused by brain edema, radiation necrosis or hemorrhage. Thus, volume rendering of the area with elevated uptake of ^{11}C-methionine superimposed on the three-dimensional surface MRI provided superior preoperative information to MRI in delineating tumor infiltration in every patient.

Determination of Motor Area from Three-Dimensional Images

Our previous PET study of motor activation of finger and oral movement in normal subjects indicated that the activation foci were observed over the pre- and post-central gyri (*23,24*). When there was not apparent deformation of cortical structure, finger movement activated the area close to the genu of the central sulcus (Fig. 2C) as reported by others (*26*). The activation focus corresponded to the area where the most

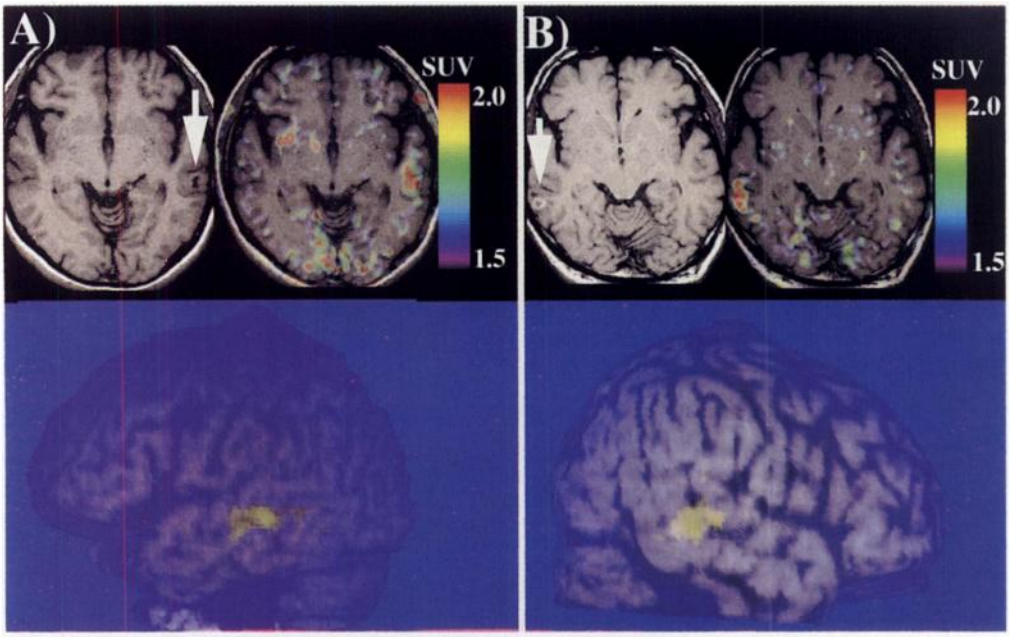

FIGURE 1. The three-dimensional surface images of area with elevated uptake of ^{11}C-methionine (SUV > 2.0) in two cases of glioma located in a single gyrus. The original axial images, from which the three-dimensional images were reconstructed. (A) A 28-yr-old woman with ganglioglioma in the left middle temporal gyrus (Patient 2) presented general convulsion, and a small lesion (arrow) was observed with MRI. (B) A 50-yr-old man with astrocytoma in the right middle temporal gyrus (Patient 11) was found to have a small lesion (arrow) when he had a health examination using MRI. In both patients, a ^{11}C-methionine study indicated the neoplastic nature of the lesions, and total removal was completed.

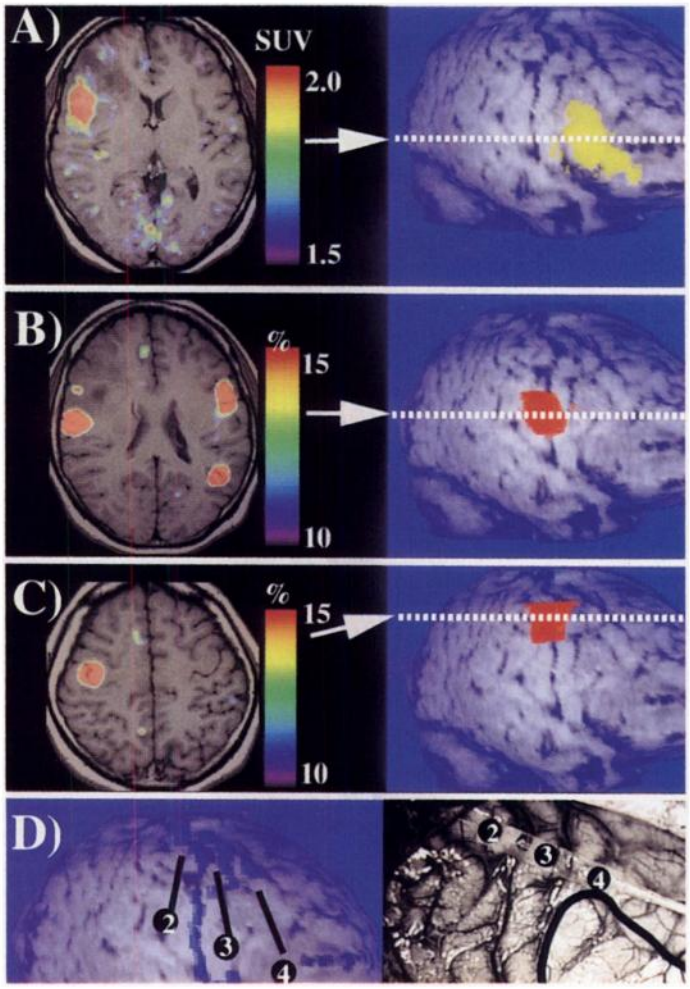

FIGURE 2. A 30-yr-old woman with right frontal astrocytoma (Patient 3). (A) The tumor area is defined as pixels that exceed 2.0 (SUV) in ^{11}C-methionine uptake on the PET images and are superimposed in a three-dimensional surface image. (B, C) Pixels that show more than a 15% elevation of PET-measured CBF during oral movement and finger movement are superimposed, respectively. (D) The correspondence between the three-dimensional surface image and the intraoperative figure. The position of the electrode, which was used for the intraoperative recording of somatosensory-evoked potential (SEP) by median nerve stimulation (*16*), is numbered in both images. The most prominent SEP were recorded in this electrode position, and it indicated that central sulcus existed between Electrode 2 and 3. Note that the center of the PET activation focus by finger movement corresponds well to this spot.

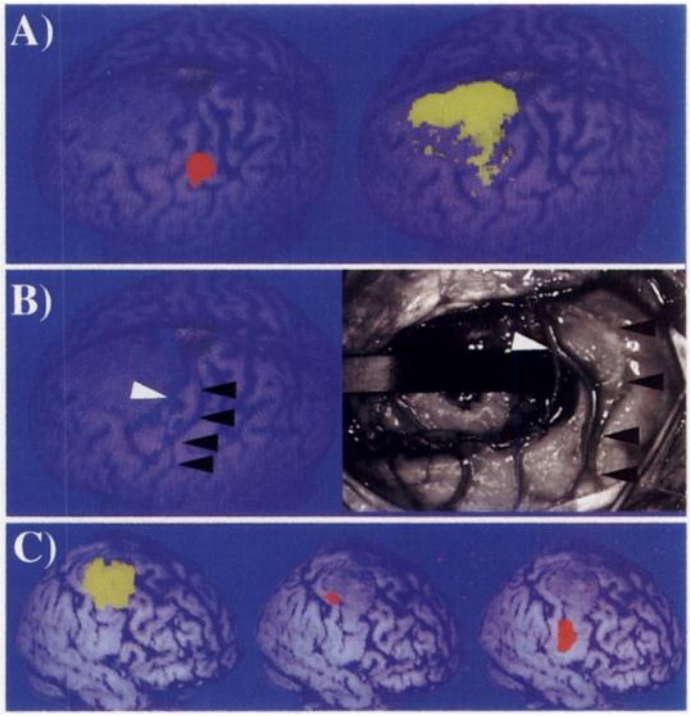

FIGURE 3. Two patients with astrocytoma in the frontal lobe. In a 60-yr-old man (Patient 16), (A) three-dimensional expression of the PET motor map in the hand area (left >15% elevation of CBF by finger movement) and PET tumor imaging (right, ^{11}C-methionine uptake (SUV) >1.8) indicated that the tumor was in the superior frontal premotor area but not in the primary motor cortex. (B) Correspondence of the three-dimensional surface image with intraoperative figure. The surface cortical vein adjacent to the tumor is a good landmark to show their correspondence. Bifurcation of the vein is indicated with a white arrowhead. The central sulcus, determined with functional mapping, is indicated by black arrowheads. (C) In a 54-yr-old man (Patient 12), the three-dimensional surface images, which were reconstructed by a similar process (^{11}C-methionine = left; finger movement = center; oral movement = right), indicated that the tumor was in the primary motor cortex. In this case, as the central sulcus is swollen and severely deviated, combined mapping of hand and face motor areas was useful to exactly determine the central sulcus.

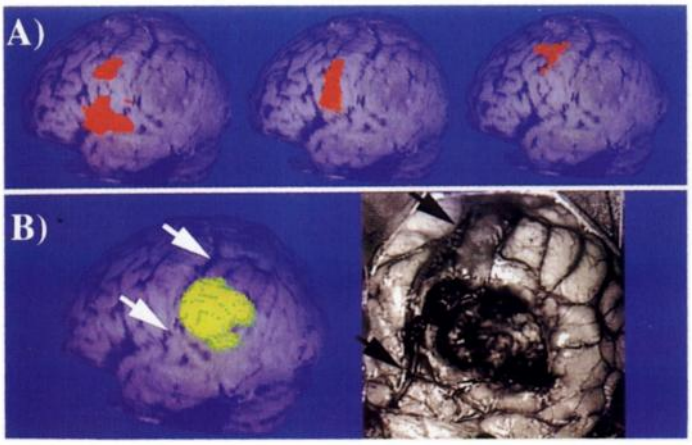

FIGURE 4. A 46-yr-old woman with a left temporoparietal glioblastoma (Patient 10). (A) Results of PET functional mapping were shown on three-dimensional surface images. As the motor and language structure is severely deviated by the mass of tumor, the activation study was performed with three kinds of tasks: word repetition (left), oral movement (center) and finger movement (right). The pixels that exceed a 10% and 15% elevation of PET-measured CBF during word repetition and motor task, respectively, were volume rendered. (B) Correspondence between the three-dimensional surface image and the intraoperative figure. A deep cortical sulcus (white arrows in left figure) with large cortical vein (black arrows in right figure) is a good landmark to indicate that the active tumor, that exceeds 2.0 (SUV) in ^{11}C-methionine uptake on the PET study (left), was completely removed (right). The patient's preoperative language and motor symptoms were ameliorated by decompression and she returned home to a good quality of life.

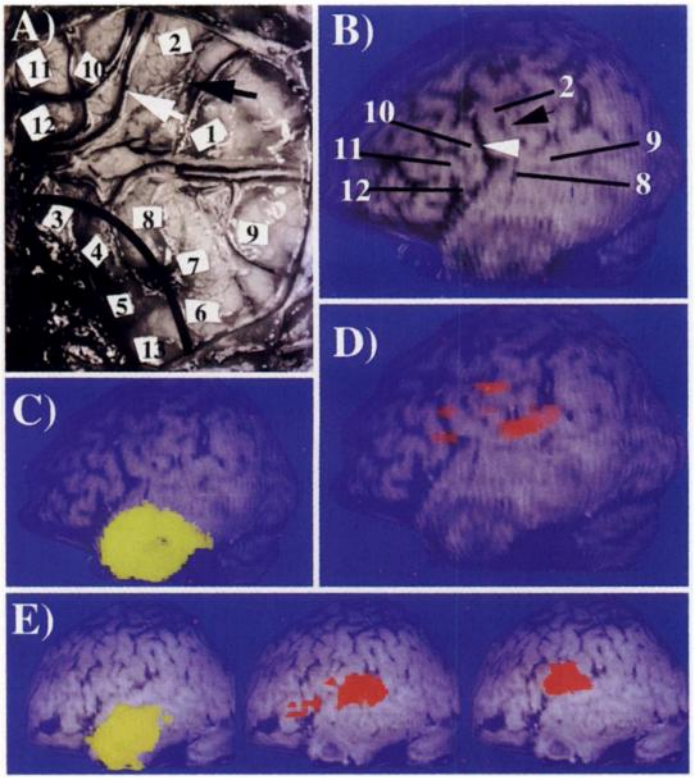

FIGURE 5. A 39-yr-old man with left temporal anaplastic astrocytoma (Patient 6). (A) Mapping of the cortex with electrical stimulation was performed on the numbered spots indicated (*14*). Stimulation of position 2 provoked twitching of the right cheek (facial motor area); stimulation of position 10 provoked speech arrest (motor language area); stimulation of position 9 provoked slight retardation of the answer (sensory language area in temporal lobe). The other positions did not cause any apparent responses (black arrow = central sulcus; white arrow = large vein on precentral sulcus; solid line = line to indicate tumor resection). The positions of numbered spots and arrows placed on (A) were superimposed in cortical surface images in (B). (C) The pixels that exceed 2.0 (SUV) in ^{11}C-methionine uptake on the PET study were volume-rendered, and (D) the pixels that show more than a 10% elevation of PET-measured CBF during word repetition are volume-rendered. (E) Similar three-dimensional images were reconstructed for a 33-yr-old woman with left temporal astrocytoma (Patient 4), who also showed swelling of the temporal lobe and deformation of parasylvian structure (^{11}C-methionine = left; word repetition = center; oral movement = right). The combined mapping of the face motor and the language areas expresses the deformation of the parasylvian structure clearly. Total removal of the tumor was completed.

prominent somatosensory-evoked potentials were recorded by the intraoperative median nerve stimulation (Fig. 2D). Therefore, we could estimate the hand motor area from three-dimensional morphological images, when there was not deformation or deviation of cortical structure. However, in cases with deformation, the correct determination of motor area was difficult with morphological images alone, and functional mapping was essential in determining it (Figs. 3 and 4). When the degree of brain swelling is severe, the combination of face and finger movement tasks was useful to trace the deviated central sulcus and to determine the spatial relationship with the tumor (Figs. 3C and 4A).

Determination of Language Area from Three-Dimensional Images

According to a previous report, the posteroinferofrontal area including Broca's area, the posterosuperotemporal area including Wernickes's area and the rolandic area related to face movement were activated by a word repetition task (*20*). All of our patients could complete the task, though some of them presented language symptoms, and a similar activation pattern was observed (Figs. 4 and 5). The activation of the temporal language cortex was consistently observed in all patients examined. The degree of activation in the frontal language cortex and that in the facial area of the motor cortex was variable. When there was no apparent deformation of cortical structure, the inferofrontal language area and parasylvian sensorimotor structure were easily defined in the surface MRI without functional mapping (Fig. 1A). When cortical structure was severely deviated by tumor, however, mapping of parasylvian language structure was useful to define the spatial relationship between the tumor and the eloquent cortex and to plan how surgical removal should be performed (Figs. 4 and 5). In one patient, with marked deformation of parasylvian structure due to swelling of the temporal lobe, the functional mapping with PET coincided with the cortical map determined with intraoperative direct cortical electrical stimulation (Fig. 5A, B, D). When mapping of the facial motor area was combined with word repetition, deformation of parasylvian functional structure was more clearly defined (Figs. 4A and 5E).

Clinical Use of Three-Dimensional Images for Operative Treatment of Glioma

Of the 16 patients examined, 12 patients underwent radical resection of the tumor. In eight patients, total or near total resection of low-grade tumor was completed. In six of the eight, three-dimensional images indicated that the tumors were located in the gyri adjacent to the primary motor or language cortex. These images also suggested that the tumors were separated from them, however, and thus total removal of the tumor could be performed successfully (Figs. 1A, 2, 3A and 5E). After total removal, transient worsening of motor or language symptom was observed in three patients (Patients 3, 9, 16). However, they fully recovered within a short interval. Four patients had malignant glioma, and maximum removal only resulted in palliative treatment (Figs. 4 and 5C). However, all of them returned home with good quality of life. When the

preoperative mass effect of the tumor was severe, decompression lead to amelioration of preoperative symptoms (Fig. 4).

In four patients, three-dimensional tumor and functional images indicated that radical resection of tumor without functional deterioration was impossible, and they were subjected to biopsy or observation. In Patient 12 (Fig. 3C) the three-dimensional images clearly showed the tumor in the primary motor cortex. We inferred that the resection of this area might cause severe deterioration of the hand and foot functions and decided not to perform radical resection. It was a good contrast with a case of the tumor in the premotor area that was radically resected only with transient deterioration of motor function (Fig. 3A, B).

In all patients presented here, our three-dimensional imaging could provide neurosurgeons with useful information, that cannot be obtained by conventional imaging, to decide on treatments for each patient.

DISCUSSION

The three-dimensional expression of brain structure and function, together with glioma imaging with radiolabeled amino acid, have substantial benefit for resection of cerebral glioma. Our experience indicates that:

1. Delineation of glioma with ^{11}C-methionine and its three-dimensional expression was one of most useful preoperative imaging techniques to identify infiltration of glial tumor in relation to cortical gyri.
2. The three-dimensional expression of the brain surface was useful in locating functioning cortex when there is no deformity of structure.
3. When the mass effect of the tumor causes deformity of the cortical structure, preoperative functional mapping of motor and/or language function was useful in determining spatial relationships between the eloquent cortex and the tumor in each patient.
4. The three-dimensional imaging protocol described here was most useful for the radical resection of a low-grade glioma adjacent to eloquent cortex.

The noninvasive mapping of cortical function has been performed mainly with PET in several institutes for investigating higher brain function in normal and diseased brain tissue (*19,21,27,28*). The method presented in this paper may be a valuable clinical application of the PET activation technique.

Recently, functional MRI with echo planer imaging also proved to be a useful imaging technique for noninvasive mapping of the brain (*29–32*). As the principle of both PET and functional MRI lies in neuro-vascular coupling (*33*), the finding obtained in our analysis with PET functional mapping also should be applicable for the same type of imaging protocol using functional MRI. Presurgical functional mapping requires a task to reveal cortical areas known to cause functional deficit by operative damage, although there are various types of activation task to map language, cognitive and motor functions. In that sense, a combination of word repetition, oral movement and simple finger movement was sufficient in locating temporal and frontal language structure and in sensorimotor area. As presurgical functional mapping is required mainly in cases in which the eloquent cortex is influenced by the mass effect of the tumor or by brain edema, the mapping technique should tolerate in such conditions. In this group of patients, we showed that PET activation with $H_2{}^{15}O$ was tolerated well with enough sensitivity under various types of pathology elicited by glioma.

The usefulness of our protocol also depends on glioma imaging with PET. The effectiveness of PET combined with a radiolabeled amino acid for the diagnosis of glioma has been established (*10–12,34–37*). Since a ^{11}C-labeled methionine uptake image is reported to be able to delineate a glioma, whether benign or malignant, better than enhanced CT or enhanced MRI (*10–12*), it is the best radiolabeled tracer for use as a preoperative imaging probe for both low-grade and malignant glial tumors. In cases of malignant glioma, ^{18}F-labeled fluorodeoxyglucose with PET and ^{201}Tl with SPECT also can be used as imaging probes. However, it should be noted that these probes may not be useful for delineating low-grade glioma (*11,38*). In cases of metastatic tumor, three-dimensional expression of the portion with gadolinium enhancement in MRI might provide sufficient information for tumor delineation. Any type of tumor imaging probe can be combined with PET functional imaging or MRI, depending on the characteristics of the tumor.

There are limitations in the use of brain surface imaging in planning tumor resection, particularly with subcortical extension. Even when the relationship between the eloquent cortex and the tumor can be assessed, the spatial relationship between the tumor and the projection fibers in relation to the sensorimotor and language functions may not be evaluated. The destruction of such fibers may cause functional deterioration even when the cortex is not damaged. Therefore, another reference such as intraoperative navigation (*39*) might be combined with our protocol. Although there are problems to be solved and long-term followup of patients is necessary to further evaluate the utility of this protocol, excellent resection of glioma and good postoperative quality of life have been achieved with this technique.

ACKNOWLEDGMENTS

This study was supported by a grant in aid for scientific research from the Ministry of Education, Science and Culture of Japan. We thank Mr. Keiichi Oda, Mr. Shinichi Ishii, Ms. Miyoko Ando and Mr. Shingo Endo for their contributions to the PET data acquisition and image analysis. We also thank Drs. Yoshiaki Takada and Tsukasa Nagaoka for their contributions to the clinical data analysis and their useful discussions.

REFERENCES

1. Levin DN, Hu X, Tan KK, et al. The brain: integrated three-dimensional display of MR and PET images. *Radiology* 1989;172:783–789.
2. Steinmetz H, Huang Y, Seitz RJ, et al. Individual integration of positron emission tomography and high-resolution magnetic resonance imaging. *J Cereb Blood Flow Metab* 1992;12:919–926.
3. Ammirati M, Vick N, Liao Y, Ciric I, Mikhael M. Effect of the extent of surgical resection on survival and quality of life in patients with supratentorial glioblastomas and anaplastic astrocytoma. *Neurosurgery* 1987;21:201–206.
4. Ciric I, Ammirati M, Vick N, Mikhael M. Supratentorial glioma: surgical consideration and immediate postoperative results. Gross total resection versus partial resection. *Neurosurgery* 1987;21:21–26.
5. Hirakawa K, Suzuki K, Ueda S, et al. Multivariate analysis of factors affecting postoperative survival in malignant astrocytoma. *J Neurooncol* 1984;2:331–340.
6. Salcman M. Radical surgery for low-grade glioma. *Clin Neurosurg* 1989;36:353.
7. Soffietti R, Chio A, Giordana MT, Vasario E, Schiffer D. Prognostic factors in well-differentiated cerebral astrocytoma in the adult. *Neurosurgery* 1989;24:686–692.
8. Winger MJ, Macdonald DR, Cairncross JG. Supratentorial anaplastic glioma in adults. The prognostic importance of extent of resection and prior low-grade glioma. *J Neurosurg* 1989;71:487–493.
9. Nagano N, Sasaki H, Aoyagi M, Hirakawa K. Invasion of experimental rat brain tumor: early morphological changes following microinjection of C6 glioma cells. *Acta Neuropathol* 1993;86:117–125.
10. Ogawa T, Shishido F, Kanno I, et al. Cerebral glioma: evaluation with methionine PET. *Radiology* 1993;186:45–53.
11. Ogawa T, Inugami A, Hatazawa J, et al. Clinical positron emission tomography for brain tumors: comparison of fluorodeoxyglucose ^{18}F and L-methyl-C^{11}-methionine. *AJNR Am J Neuroradiol* 1996;17:345–353.
12. Tovi M, Lilja A, Bergstrom M, Ericsson A, Bergstrom K, Hartman M. Delineation of gliomas with magnetic resonance imaging using Gd-DTPA in comparison with computed tomography and positron emission tomography. *Acta Radiol* 1990;31:417–429.
13. Penfield W, Roberts L. *Speech and brain mechanism*. Princeton, NJ: Princeton University Press; 1959.

14. Ojemann GA. Cortical organization of language. *J Neurosci* 1991;11:2281–2287.
15. McCarthy G, Allison T, Spencer DD. Localization of the face area of human sensorimotor cortex by intracranial recording of somatosensory evoked potentials. *J Neurosurg* 1993;79:874–884.
16. King RB, Shell GR. Cortical localization and monitoring during cerebral operations. *J Neurosurg* 1987;67:210–219.
17. Herscovitch P, Markham J, Raichle ME. Brain blood flow measured with intravenous $H_2{}^{15}O$. I. Theory and error analysis. *J Nucl Med* 1983;24:782–789.
18. Raichle ME, Martin WRW, Herscovitch P, Mintun MA, Markham J. Brain blood flow measured with intravenous $H_2{}^{15}O$. II. Implementation and validation. *J Nucl Med* 1983;24:790–798.
19. Colebatch JG, Deiber M, Passingham RE, Friston KJ, Frackowiak SJ. Regional cerebral blood flow during voluntary arm and hand movement in human subjects. *J Neurophysiol* 1991;65:1392–1401.
20. Ohyama M, Senda M, Kitamura S, Ishii K, Mishina M, Terashi A. Role of nondominant hemisphere and undamaged area during word repetition in poststroke aphasics. A PET activation study. *Stroke* 1996;27:897–903.
21. Petersen SE, Fox PT, Posner MI, Mintun M, Raichle ME. Positron emission tomographic studies of the cortical anatomy of single-word processing. *Nature* 1988;331:585–589.
22. Fox PT, Mintun MA, Reiman EM, Raichle ME. Enhanced detection of focal brain responses using intersubject averaging and change-distribution analysis of subtracted PET images. *J Cereb Blood Flow Metab* 1988;8:642–653.
23. Senda M, Kanno I, Yonekura Y, et al. Comparison of anatomical standardization methods regarding the sensori-motor foci localization and between-subject variation in $H_2{}^{15}O$ PET activation, a three-center collaboration study. *Ann Nucl Med* 1994;8:201–207.
24. Senda M. Mapping cortical functions using PET activation technique. In: Sugishita M, ed. *New horizons in neuropsychology*. Amsterdam, The Netherlands: Elsevier Science; 1994:23–34.
25. Uemura K, Toyama H, Kimura Y, Nishina M, Senda M, Uchiyama A. Edge enhancing filter using modified fractal dimension for automatic edge detection of brain MRI. *J Cereb Blood Flow Metab* 1995;15:S605.
26. Rumeau C, Tzourio N, Murayama N, et al. Location of hand function in the sensorimotor cortex: MR and functional correlation. *AJNR: Am J Neuroradiol* 1994;15:567–572.
27. Grafton ST, Woods RP, Mazziotta JC, Phelps ME. Somatotopic mapping of the primary motor cortex in humans: activation studies with cerebral blood flow and positron emission tomography. *J Neurophys* 1991;66:735–743.
28. Rumsey JM, Andreason P, Zametkin AJ, et al. Failure to activate the left temporoparietal cortex in dyslexia. An ^{15}O positron emission tomographic study. *Arch Neurol* 1992;49:527–534.
29. Binder JR, Rao SM, Hammeke TA, et al. Lateralized human brain language systems demonstrated by task subtraction functional magnetic resonance imaging. *Arch Neurol* 1995;52:593–601.
30. Demb JB, Desmond JE, Wagner AD, Vaidya CJ, Glover GH, Gabrieli JD. Semantic encoding and retrieval in the left inferior prefrontal cortex: a functional MRI study of task difficulty and process specificity. *J Neurosci* 1995;15:5870–5878.
31. McCarthy G, Blamire AM, Rothman DL, Gruetter R, Shulman RG. Echo-planar magnetic resonance imaging studies of frontal cortex activation during word generation in humans. *Proc Natl Acad Sci USA* 1993;90:4952–4956.
32. Sakai K, Watanabe E, Onodera Y, et al. Functional mapping of the human somatosensory cortex with echo-planar MRI. *Magnet Res Med* 1995;33:736–743.
33. Villringer A, Dirnagl U. Coupling of brain activity and cerebral blood flow: basis of functional neuroimaging. *Cerebrovasc Brain Met Rev* 1995;7:240–276.
34. Ishiwata K, Kubota K, Murakami M, et al. Re-evaluation of amino acid PET studies: can the protein synthesis rates in brain and tumor tissues be measured in vivo? *J Nucl Med* 1993;34:1936–1943.
35. Derlon JM, Bourdet C, Bustany P, et al. Carbon-11-L-methionine uptake in gliomas. *Neurosurgery* 1989;25:720–728.
36. Mineura K, Sasajima T, Suda Y, Kowada M, Shishido F, Uemura K. Amino acid study of cerebral gliomas using positron emission tomography—analysis of (^{11}C-methyl)-L-methionine uptake index. *Neurol Med Chir Tokyo* 1990;30:997–1002.
37. Sato K, Kameyama M, Ishiwata K, Hatazawa J, Katakura R, Yoshimoto T. Dynamic study of methionine uptake in glioma using positron emission tomography. *Eur J Nucl Med* 1992;19:426–430.
38. Dierckx RA, Martin JJ, Dobbeleir A, Crols R, Neetens I, De Deyn PP. Sensitivity and specificity of ^{201}Tl single-photon emission tomography in the functional detection and differential diagnosis of brain tumors. *Eur J Nucl Med* 1994;21:621–633.
39. Golfinos JG, Fitzpatrick BC, Smith LR, Spetzler RF. Clinical use of a framelesssteereotactic arm: results of 325 cases. *J Neurosurg* 1995;83:197–205.

Graphical Analysis of 6-Fluoro-L-Dopa Trapping: Effect of Inhibition of Catechol-O-Methyltransferase

J.E. Holden, D. Doudet, C.J. Endres, G.L-Y. Chan, K.S. Morrison, F.J.G. Vingerhoets, B.J. Snow, B.D. Pate, V. Sossi, K.R. Buckley and T.J. Ruth

Department of Medical Physics, University of Wisconsin, Madison, Wisconsin; and Neurodegenerative Disorders Centre and TRIUMF, University of British Columbia, Vancouver, British Columbia

Graphical methods to analyze tracer time-course data allow reliable quantitation of the rate of incorporation of tracer from plasma into a "trapped" kinetic component, even when the details of the kinetic model are unknown. Applications of the method over long time periods often expose the slow reversibility of the trapping process. In the extended graphical method, both trapping rate and a presumed first-order loss rate constant are estimated simultaneously from the time-course data. **Methods:** We applied the extended graphical method to 6-fluoro-L-dopa (6-FD), simultaneously estimating the rate of uptake (K_i) and the rate constant for loss from the trapped component (k_{loss}) in a single fitting procedure. We applied this approach to study the effects of two catechol-O-methyl-transferase inhibitors on the kinetics of 6-FD in cynomolgus monkeys. **Results:** Inhibition of peripheral O-methylation with either inhibitor, confirmed by high-performance liquid chromatography analysis of labeled compounds in arterial plasma, had no significant effect on K_i, in agreement with previously reported studies. In contrast, tolcapone, a catechol-O-methyl-transferase inhibitor, having central effects in addition to peripheral effects at the dosage used, decreased k_{loss} by 40% from control values ($p < 0.002$), whereas nitecapone, which has no known central activity, had no significant effect. **Conclusion:** This method provides insight into the neurochemical basis for the kinetic behavior of 6-FD in both health and disease and may be used to define the action of centrally active drugs that influence the metabolism of dopamine.

Key Words: 6-fluoro-dopa; reversible trapping; extended graphical method; PET; COMT inhibition

J Nucl Med 1997; 38:1568–1574

After the early work of Garnett et al. (*1*), PET with the tracer 6-fluoro-L-dopa (6-FD), labeled with ^{18}F, became a recognized and validated technique for the assessment of nigrostriatal function (*2*). The 6-FD is taken up into the nigrostriatal nerve terminals and decarboxylated to 6-fluorodopamine (6-FDA) (Fig. 1). Like dopamine, 6-FDA cannot cross the blood–brain barrier and is trapped. In all data reduction approaches, this apparently irreversible accumulation of label in the striatum is clearly identified. In particular, application of the graphical method (*3*) to data collected in the first 2 hr following bolus administration of 6-FD invariably yields straight-line behavior, in keeping with such irreversible trapping. However, extension of the measurements beyond 2 hr shows that the assumption of

Received Jun. 27, 1996; revision accepted Nov. 14, 1996.

For correspondence or reprints contact: James E. Holden, PhD, 1530 Medical Sciences Center, 1300 University Avenue, Madison, WI 53706.